

# THEORETICAL AND NUMERICAL ESTIMATION OF SOUND POWER FROM OUT OF PLANE MODES OF A FREE ANNULAR CIRCULAR PLATE HAVING PARABOLICALLY VARYING THICKNESS

ABHIJEET CHATTERJEE<sup>1</sup>, VINAYAK RANJAN<sup>2</sup> & MOHAMMAD SIKANDAR AZAM<sup>3</sup>

<sup>1</sup>Department of Mechanical Engineering, Indian Institute of Technology (ISM), Dhanbad, India

<sup>2</sup>Department of Mechanical and Aerospace Engineering, Bennett University, Greater Noida, Uttar Pradesh, India

<sup>3</sup>Department of Mechanical Engineering, Indian Institute of Technology (ISM), Dhanbad, India

## ABSTRACT

*In this study, the sound radiation characteristic of an annular circular plate with parabolically varying thickness with different taper ratios and different excitation locations are analysed. The mass of the plate is kept constant for all thickness variations. Rayleigh integral is applied to determine the acoustic radiation coupling between interacting structural modes of the plate. Further, this method is applied to determine the self and mutual radiation from out of plane  $(m, n)^{th}$  modes. The same problem is also solved by ANSYS to draw the comparison. The sound power is generated by harmonic force at different excitation locations is calculated from self and mutual radiation. It is observed that the mutual radiation due to modal coupling exists only when two out of plane structural modes have same  $n$ . Finally, excitation location with different taper ratios provides us a solution for peak sound power actuation as well as peak sound power reduction.*

**KEYWORDS:** Thick Annular Plate, Natural Frequencies, Taper Ratio, Sound Power, Tapered Plate & Parabolic Varying Thickness

**Received:** Jul 27, 2018; **Accepted:** Aug 17, 2018; **Published:** Jan 14, 2019; **Paper Id.:** IJMPERDFEB201937

## INTRODUCTION

Plate with parabolic varying thickness has been used for many engineering applications. They are mostly used in diaphragms and deck plates in launch vehicles, telephone industry, diaphragms of turbines, naval structures, optical systems, constructions of ships, automobiles and other vehicles, aircrafts/missiles, nuclear reactors, space shuttle, sound emitters and receivers, circular ports and panels, pneumatic pumps, cochleae, gongs and cymbals etc[1-9]The tapered plate with different arbitrarily varying thickness is found to have significantly greater resistance to bending, buckling and vibration in comparison to the corresponding plates of uniform thickness. Hence, it has drawn a wide attention in this field of acoustic and vibration. However, the plates with a different arbitrarily varying thickness can alter the dynamic characteristic of the structure due to change in stiffness. Therefore, for practical design, it is necessary to study the vibration and acoustic behaviour of such tapered plates. Among existing literature, several researchers have investigated the sound radiation behaviour of the circular or annular plate. Lee and Singh[10] determined the sound radiation from out-of-plane modes of uniform thickness annular circular plate using thin and thick plate theories. Thompson [11] determined the mutual and self-radiation impedances both for annular and elliptical pistons using Bouwkamp integral. Levine and Leppington [12] analysed

the sound power generation of a circular plate of uniform thickness using the exact integral representation. Rdzanek and Engel [13] determined the acoustic power output of a clamped annular plate using asymptotic formula. Wodtke and Lamancusa [14] minimized the acoustic power of circular plates of uniform thickness using the damping layer placement. Wanyama [15] studied the acoustic radiation from linearly-varying circular plates using Rayleigh surface integral and surface integration method. Lee and Singh [16] used the flexural and radial modes of a thick annular plate to determine the self and mutual radiation using the modal expansion technique. Cote et al. [17] studied the vibro acoustic behaviour of an unbaffled rotating disk using Rayleigh Ritz approach. Jeyraj [18] used an isotropic plate with arbitrarily varying thickness to determine its vibro-acoustic behaviour using finite element method. Ranjan and Ghosh [19] studied, forced response of thin plates of uniform thickness with attached discrete dynamic absorbers using finite element method. Bipin et al. [20] analysed an isotropic plate with attached discrete patches and point masses with different thickness variation with different taper ratios to determine its vibro acoustic response using Rayleigh integral and finite element method. Lee and Singh [21] investigated the annular disk acoustic radiation using structural modes through analytical formulations using far field and radiation impedance approach. Rdzanek et al [22] investigated the sound radiation and sound power of a planar annular membrane for axially-symmetric free vibrations using both Bouwkamp integral and Cauchy's theorem.

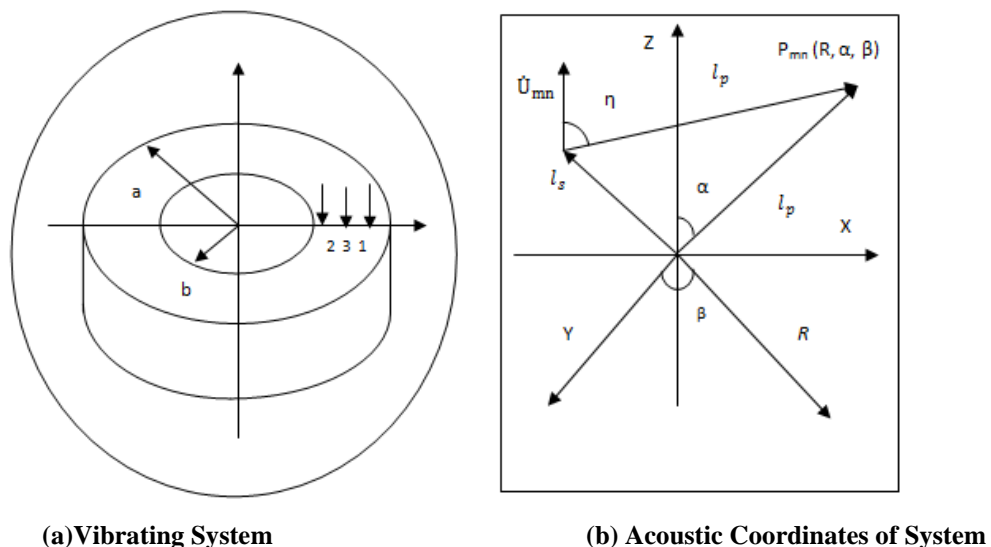


**Figure 1: Represents the (a) Vibrating System (b) Acoustic Coordinates of System to Determine the Acoustic Radiation**

Nakayama et al [23] investigated the acoustic radiation of a circular plate for a single sound pulse. Lee and Singh [24] used a simplified disk brake rotor to investigate the acoustic radiation through a semi-analytical method. Thompson et al. [25,26] analysed the modal approach for different boundary conditions to calculate the average radiation efficiency of a rectangular plate. Rayleigh [27] determined the sound radiation from flat finite structures. Maidanik [28] analysed the total radiation resistance for ribbed and simple plates using a simplified asymptotic formulation. Hecki [29] analysed the acoustic power using wave number domain and Fourier transforms. Williams [30] determined the wave number as a series in ascending power to estimate the sound radiation from planar source. Keltie and Peng [31] analysed the sound radiation using the cross-modal coupling from a plane using Heckl's power integral. Snyder and Tanaka [32] demonstrated the importance of cross-modal contributions for a pair of modes through total sound power output using modal radiation efficiency.

Review of the literature suggested that a study of sound radiation behaviour due to self and mutual radiation of a circular, annular plate having a parabolic varying thickness with different taper ratios and exciting force at different locations and keeping the mass of the plate constant with free-free boundary condition is not reported. Therefore, In this paper the self and mutual radiation from out of plane modes of an annular circular plate with free - free boundary condition having parabolically varying thickness with different taper ratios are analysed keeping the mass of the plate constant under time-varying harmonic excitation.

### **Mathematical Modelling and Analysis Procedure Free Vibration of Plate**

The eigen value problem for  $\omega^2$  due to the natural frequency and modes shape of the plate is given by

$$([K] - \omega^2 [M])\psi_{mn} = 0 \quad (1)$$

Where [M] is known to be the mass matrix and [k] is known to be the stiffness matrix while  $\psi_{mn}$  is considered to be the mode shape of plate and the corresponding natural frequency of the plate is  $\omega$  in rad/sec.

The non-dimensional frequency parameter ' $\lambda^2$ ' is given by

$$\lambda^2 = \omega a^2 \sqrt{\frac{\rho h}{D}} \quad (2)$$

Where D is considered to be the flexure rigidity  $= \frac{Eh^3}{12(1-\nu^2)}$ , E is the Young's modulus of elasticity,  $\nu$  is the Poisson's ratio, h is the thickness of the plate and  $\rho$  is known to be the density of plate.

### **Analytical and Numerical Formulation for Acoustic Radiation from Annular Circular Plate**

It is considered that an annular circular plate of inner radius 'b' and outer radius 'a' in flexural vibration is set on flat rigid baffle having infinite extent as reported in Figure 1. Acoustic scattering of the edges of a vibrating structure is neglected in this study. If P be the self sound pressure amplitude,  $S_s$  be the surface of the sound source,  $q$  be the Green function in free field,  $l_s$  and  $l_p$  be the position vectors of source and receiver and the surface normal vector at  $l_s$  be  $f$ , then structure sound radiation can be obtained by Rayleigh integral [10] as given by

$$P(l_p) = \int_{S_s} \left( \frac{\partial q}{\partial f}(l_p, l_s) P(l_p) - \frac{\partial P}{\partial f}(l_s) q(l_p, l_s) \right) ds(l_s) \quad (3)$$

The sound pressure, radiated from non-planar source in far and free field environment based on plane wave approximation can be expressed by

$$P(l_p) = \frac{\rho_0 c_0 B}{4\pi} \int_{S_s} \frac{e^{iB|l_p - l_s|} \dot{U}(l_s)}{|l_p - l_s|} (1 + \cos \eta) dS \quad (4)$$

If  $\rho_0$  be the mass density of air,  $c_0$  be the speed of sound in air, B be the corresponding acoustic wave number, and  $\dot{U}$  and  $\dot{u}_z$  be the corresponding vibratory velocity amplitude and spatial dependent vibratory velocity amplitude in the z direction at  $l_s$ , then from a normal plane [10], the modal sound pressure  $P_{mn}$  for an annular plate with (m, n)<sup>th</sup> mode is obtained from simplifying Eq.(4) with Hankel transform and is expressed by

$$P_{mn}(R, \alpha, \beta) = \frac{\rho_0 c_0 B e^{iB_{mn} R_d}}{2R_d} \cos n\beta (-i)^{n+1} A_n \left[ \dot{u}(l) \right] (1 + \cos \eta) \quad (5)$$

$$A_f \left[ \dot{u}(l) \right] = \int_0^\infty \dot{u}(l) J_n(B_l l) l dl, B_l = B \sin \theta; R_d = |l_p - l_s| \quad (6)$$

Where,  $m$  represents the number of nodal circles in the plate and  $n$  represent the number of nodal diameters in the plate.  $J_n$  is Bessel function of order  $n$ ,  $(\alpha, \beta)$  are the cone and azimuthal angles of the observation positions, respectively,  $\eta$  is the angle between the surface normal vector and the vector from source position to receiver position, and  $A$  is the Hankel transform. According to the far field condition,  $R_d$  in the denominator is approximated by  $R$  where  $R = |l_p|$  is considered to be radius of the sphere. Considering on a sphere  $S_v$  the observation positions are represented by some points having equal angular increments  $(\Delta\phi, \Delta\alpha)$ . If ' $\Delta\phi$ ' represents the small increment in the circumferential direction of the plate, at all of the observation positions, the sound pressures is given by Eqs. (4-6).

The modal sound power  $S_{mn}$  for the  $(m, n)^{th}$  mode<sup>10-16</sup> from the far-field is given by

$$S_{mn} = (D_{mn} S_v)_s = \frac{1}{2} \int_0^{2\pi} \int_0^\pi \frac{P_{mn}^2}{\rho_0 c_0} R^2 \sin \alpha d\alpha d\beta \quad (7)$$

Where the acoustic intensity is represented by  $D_{mn}$  and area of the control surface is represented by  $S_v$ . The radiation efficiency  $\sigma_{mn}$  of the plate<sup>10</sup> is given by

$$\sigma_{mn} = \frac{S_{mn}}{\left| \dot{u}_{mn} \right|_{ts}^2}, \left| \dot{u}_{mn} \right|_{ts} = \frac{1}{2\pi(a^2 - b^2)} \int_b^a \int_0^{2\pi} \dot{U}^2 d\phi dl \quad (8)$$

Where, for the two normal surfaces of the plate the spatially average r.m.s velocity is represented by  $|\dot{u}_{mn}|_{ts}$ . Considering the plate thickness ( $h$ ) effect, the sum of sound radiations<sup>16</sup> from two normal surfaces of the plate at  $(Z = 0.5h$  and  $-0.5h)$  will represent the modal sound power which can be given by

$$P_{mn}(R, \alpha, \beta) = (1 + \cos \alpha) P_{mn}^s(R, \alpha, \beta) + (1 - \cos \alpha) P_{mn}^o(R, \alpha, \beta) \quad (9)$$

$$P_{mn}^s(R, \alpha, \beta) = \frac{\rho_0 c_0 B_{mn} e^{iB_{mn} R}}{2R} e^{-iB_{mn} \left(\frac{h}{2}\right) \cos \alpha} \cos n\beta (-i)^{n+1} A_n \left[ \dot{U}(l) \right] \quad (10)$$

$$P_{mn}^o(R, \alpha, \beta) = \frac{\rho_0 c_0 B_{mn} e^{iB_{mn} R}}{2R} e^{-iB_{mn} \left(\frac{h}{2}\right) \cos \alpha} \cos n(\beta + \phi) (-i)^{n+1} A_n \left[ \dot{U}(l) \right] \quad (11)$$

Where, the corresponding acoustic wave number of the  $(m, n)^{th}$  mode is represented by  $B_{m,n}$ ,  $s$  and  $o$  in Eq. (10-11) represent source side and opposite to source side. If several modes are excited the total sound power for a frequency can be divided into two groups. First, power from self radiation of individual modes and second power from the mutual radiation between two or more structural modes. The modal coupling may be either due to two  $(m, n)$  modes or two radial modes as well as between structural mode  $(m, n)$  and radial modes ( $r$ ). However, in this paper, the mutual radiation due to modal coupling between two out of plane structural modes  $(m, n)$  and  $(m^1, n^1)$  is considered and these two modes have same  $n$ . The total acoustic power [16] generated by the coupling between the  $(m, n, r)^{th}$  mode and  $(m^1, n^1, r^1)^{th}$  mode is given by

$$S_{mnr}^{m^1 n^1 r^1} = \frac{1}{2} \int_0^{2\pi} \int_0^{\frac{\pi}{2}} \frac{P_{mnr} P_{m^1 n^1 r^1}^*}{\rho_0 c_0} R^2 \sin \alpha d\alpha d\beta \quad (12)$$

Where,  $P^*$  is the mutual sound pressure amplitude.  $S_{mnr}^{m^1 n^1 r^1}$  is the power from self radiation when  $m = m^1$ ,  $n = n^1$  and  $r = r^1$  otherwise  $S_{mnr}^{m^1 n^1 r^1}$  is due to the mutual radiation between  $(m, n, r)^{th}$  modes and  $(m^1, n^1, r^1)^{th}$  modes.

For numerical analysis, we have used ANSYS as a tool for computation. The plate is modelled in ANSYS Plane 185 with 8 brick nodes and having three degrees of freedom at each node. FLUID 30 and FLUID130 elements are used to create the acoustic medium environment around the plate. For fluid-structure interaction FLUID 30 is used. For the surface on outer sphere, FLUID 130 elements are created by imposing a condition of infinite space around the source and to prevent the back reflection of sound waves to the source. After proper convergence of modelling for thickness variation, the numbers of elements and nodes come out to be 14653 and 3618 respectively. A concentrated harmonic force of amplitude 1N is applied at three different exciting locations 1, 2 and 3 to vibrate the mild steel annular circular plate as shown in Figure 1. The position chosen are 0.0069 m, 0.0345 m and 0.0621m for excitation location 1, 2 and 3 respectively. Consider the air medium where the plate undergoes vibration with air density  $\rho_0 = 1.21 \text{ kg/m}^3$ . At  $20^\circ\text{C}$ , the speed of sound  $c_0$  of air is taken as 343m/s. The structural damping coefficient of the plate is assumed as 0.01.

## THICKNESS VARIATION OF THE PLATE

In this paper, a parabolically decreasing thickness variation in radial direction for free free thick annular circular plate is considered for analysis and is reported in Figure 2. The radial direction is considered for thickness variation by keeping the total mass of the plate constant. In radial direction the plate thickness is given by  $h_x = h [1 - T_x \{f(x)\}^n]$ , where 'h' is the maximum thickness of the plate and  $f(x)$  is considered to be an arbitrary function of ordinate x.

Where,

$$f(x) = \begin{cases} 0, & x = b \\ 1, & x = a \end{cases} \quad \text{and} \quad f(x) = \frac{x-b}{a-b} \quad \text{where } b < x < a \quad (13)$$

And the taper parameter or taper ratio ( $T_x$ ) is given by

$$T_x = \left( 1 - \frac{h_{\min}}{h} \right) \quad (14)$$

The equation for parabolically decreasing thickness variation (Figure 2) is given by

$$h_x = h \left\{ 1 - T_x \left( \frac{x-b}{a-b} \right)^n \right\} \quad (15)$$

Where  $n=2$  for parabolic profile. The total volume of the plate is kept constant and is given by

$$\text{Volume} = \pi(a^2 - b^2)h = \int_b^a (a^2 - b^2)h_x dx \quad (16)$$

In this paper, the effect of force excitation locations on sound power level, average radiation efficiency and peak sound power level from out of plane modes of free-free annular circular plate with decreasing parabolic varying thickness

with different taper ratios of 0.25, 0.50 and 0.75 are analysed keeping the mass of the plate constant. The dimension and the material properties of an annular circular tapered plate are reported in Table 1. Rayleigh integral has been used for sound power calculation and ANSYS has been used as a tool for computation.

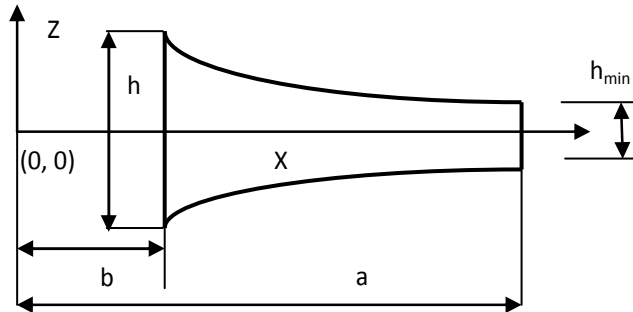


Figure 2: Plate with Parabolic Varying Thickness Variations

## RESULTS AND DISCUSSIONS

### Validation of Modal Frequency and Acoustic Power Calculation

In this paper, the modal frequency of the thick annular circular plate is validated with the existing result of Lee and Singh [10]. From Table 2 it is clearly understood that the results obtained in this study is in good and good agreement with the existing literature [10]. For acoustic power calculation the force excitation at different locations for two out of plane modes  $(m, n)$  and  $(m^1, n^1)$  are considered. The total power generated, including self power and mutual power due to modal coupling of two out of plane modes  $(m, n)$  and  $(m^1, n^1)$  is calculated both analytically and numerically. The calculated result of total power due to the force excitation at different locations is validated with the published experimental results of the existing literature [10]. A good and well agreement of result is seen as reported in Figure 3.

Table 1: The Dimension and the Material Properties of the Annular Circular Tapered Plate

Dimension of the Plate	Annular Circular Tapered Plate
Radii ratio, $(b/a)$	0.54
Thickness radii ratio, $(h/a)$	0.21
Density, $\rho$ ( $\text{kg/m}^3$ )	7905.9
Young's modulus, $E$ (GPa)	218
Poisson's ratio, $\nu$	0.305

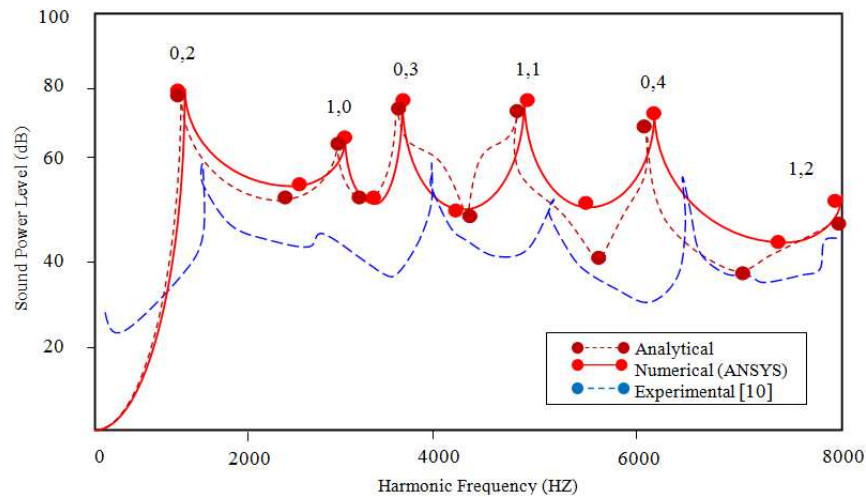
Table 2: Validation and Comparison of Frequency Parameter  $\lambda^2$  of Uniform Isotropic Annular Circular Plate Obtained in Present Work with that of Lee and Singh [10]

Plate	Mode	Non Dimensional Frequency Parameter, $\lambda^2$	
		Lee and Singh [10]	Present Work
Parabolic Plate $b/a = 0.54$ $h/a = 0.21$	(0,2)	3.82	3.83
	(1,0)	8.85	8.82
	(0,3)	10.59	10.02
	(1,1)	15.42	13.70

**Table 3: Self and Mutual Radiation Power (Db) of Selected Structural Modes of Uniform Thick Annular Plate with Free - Free Boundary Condition**

(m,n)		Sound Power Level (dB)
1 <sup>st</sup> Mode	2 <sup>nd</sup> Mode	
(0, 2)	(0, 2)	82
(1, 0)	(1, 0)	64
(0, 3)	(0, 3)	79
(1, 1)	(1, 1)	78
(0, 4)	(0, 4)	75
(1, 2)	(1, 2)	56

In this paper, the total power generated, including self power and mutual power due to modal coupling of two out of plane structural modes  $(m, n)$  and  $(m^1, n^1)$  is calculated neglecting radial mode are = 0 in Eq.12. The mutual radiation due to modal coupling of two out of plane modes  $(m, n)$  and  $(m^1, n^1)$  exist only when two out of plane structural modes have same  $n$  i.e.  $n = n^1$ . The self and mutual radiation powers due to two interacting modes are shown in Table 3.



**Figure 3: Analytical, Experimental and Numerical Comparison of Sound Power Level for Uniform Plate**

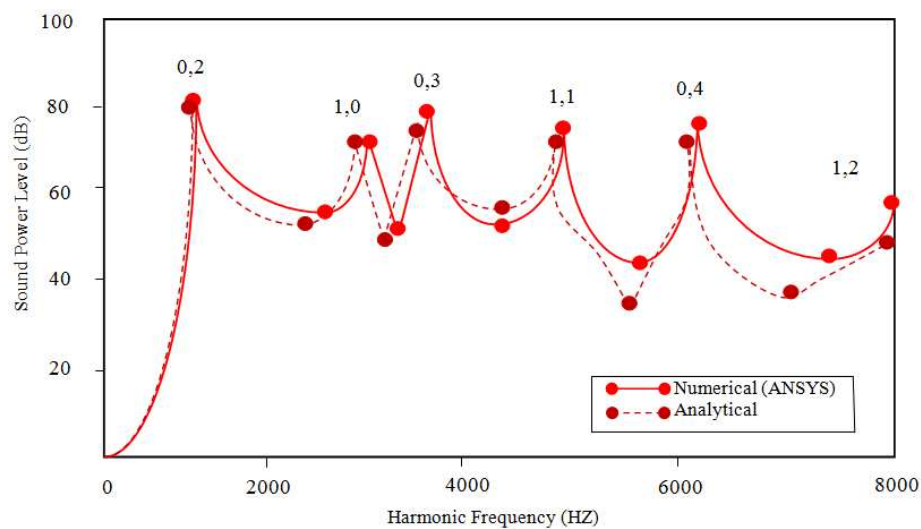


**Figure 4: Analytical and Numerical Comparison of Sound Power Level for Plate with Excitation Location 1 Having Parabolic Decreasing Thickness Variation for Taper Ratio  $T_x = 0.75$**



### Acoustic Response Solution of Plate With Parabolic Varying Thickness for Different Taper Ratio $T_x$ .

The sound power level (dB, reference =  $10^{-12}$  watts) due to self and mutual radiation of annular circular plate with parabolically decreasing thickness variation due to transverse vibration for different taper ratios is investigated by applying a concentrated load under time-varying harmonic excitations. A harmonic frequency range of 0-8000 Hz is taken to determine the sound radiation characteristic. Figure 4 shows the sound radiation behaviour for annular plate obtained analytically and numerically for taper ratio  $T_x = 0.75$  for excitation location 1 and for different modes.

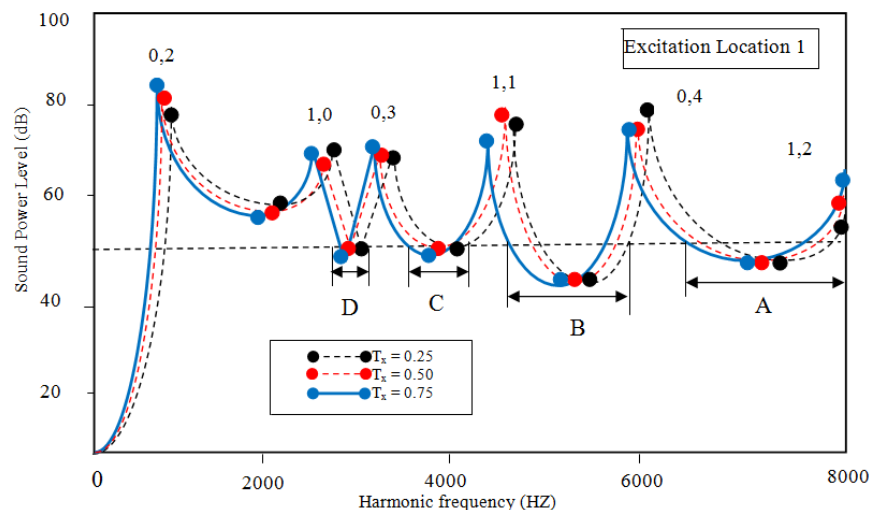


**Figure 5: Numerical Comparison of Sound Power Level for Plate Having Parabolically Decreasing Thickness Variation with Different Taper Ratio  $T_x$  under Excitation Location 1**

A well and good agreement of results is seen in comparison of sound power level as depicted in Figures 4, 5, 6 & 7 show the sound radiation behaviour for different taper parameters for different excitation locations and for different modes obtained numerically. From Figures (5-7), it is observed that for very low excitation frequency rises 200 Hz, different excitations locations and stiffness variation due to taper ratio do not have a significant effect on sound power radiation for free-free boundary condition. However, when the excitation frequency increases beyond 200 HZ and rises the first peak, then sound power level is higher for higher taper ratio for excitation location 1 and variation of sound power level due to variation of peaks for different taper ratios is observed for excitation locations 2 and 3 at a given forcing frequency. Further, different modes do influence the sound power peaks as evident from Figures 5-7. Sound power level peak obtained for different modes does not remain same for different taper ratios. However sounds power level peaks do shift towards lower frequency as taper ratio increases and a different taper ratio alter its stiffness at higher forcing frequency. From Figures (5-7), it is observed that excitation locations and mode shapes variation have a significant effect on sound power level in comparison to stiffness variation for different taper ratios. For taper ratio,  $T_x = 0.75$ , the highest sound power level 82 dB is obtained for excitation location 1 in Figure 5 while for excitation locations 2 and 3, the highest sound power level obtained are 79 dB and 78 dB respectively as reported in Figures. 6 & 7. Further it is obtained from the Figure 5 that sound power level rises 40 dB, we do not get any broad range of frequencies for different taper ratio for excitation location 1. However, for sound power level between (40 – 50) dB, we get a broad range of frequencies in different frequency bands A, B, C, and D as reported in Figure 5. Further, it is observed that for sound power level between (40 – 50) dB in frequency band C and D, taper ratio  $T_x = 0.75$  is available design alternative while in frequency bands A



and B, all taper ratios may be opted as a design solution for sound power level. From Figure 6, it is apparent that when excitation location changes to 2 i.e. towards inner radius, and when sound power level, rises 40 dB we get all broad range of frequencies in frequency bands A only. But for sound power level between (40 – 50) dB, we get a wider range of frequency bands, C, D and E for different taper ratios. From Figure 7, it is noted that when the force excitation changes to location 3 (mid excitation) then for sound power level rises 40 dB, we get all broad range of frequencies in frequency bands A and B only. But, for sound power level between (40 – 50) dB, we get a broader range of frequency bands C, D and E for all taper ratios. From Figures 5-7, it is clear that excitation locations play a significant role in getting a broader range of frequencies in different frequency bands to sound power level. It is interesting to note that for sound power level rises 40 dB, mid excitation (excitation location 3) provides design options in a broad frequency range. Also, modes have significant influence on sound power level as evident from Figures (5-7). However stiffness contributions due to various taper ratios have very limited impact on sound power level in comparison to that of excitation locations.

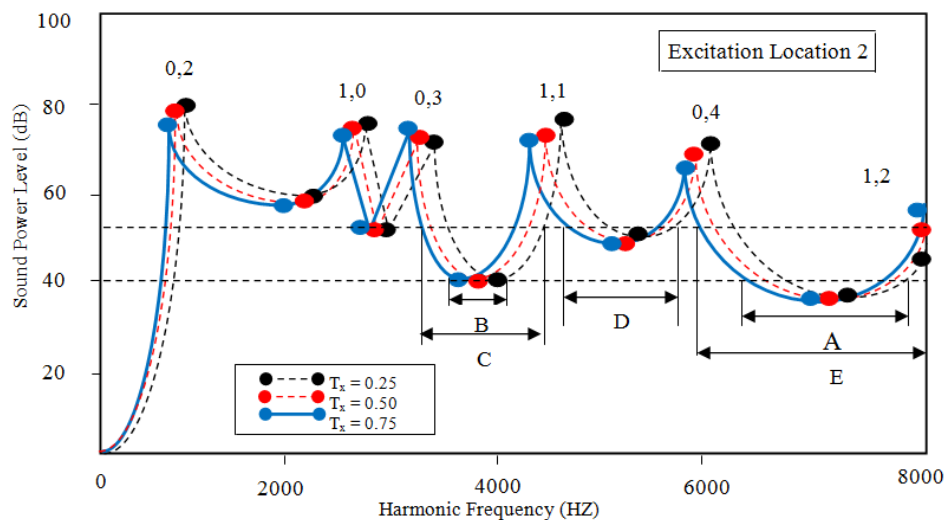


**Figure 6: Numerical Comparison of Sound Power Level for Circular Annular Plate Having Parabolically Decreasing Thickness Variation with Different Taper Ratio  $T_x$  under Excitation Location 2**

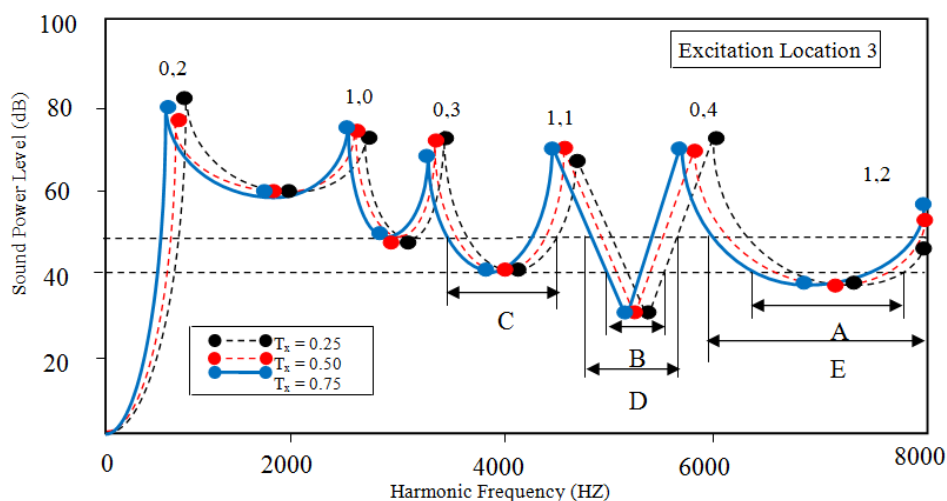


**Figure 7: Numerical Comparison of Sound Power Level for Circular Annular Plate Having Parabolically Decreasing Thickness Variation with Different Taper Ratio  $T_x$  Under Excitation Location 3**

Figure 8 shows the numerical comparison of sound power level for circular annular plate having parabolic decreasing thickness variation for different excitation locations and for different taper ratios  $T_x$ . From Figure 8, it is observed that for excitation frequency rises 200 Hz, plate with parabolically decreasing thickness variation with different excitation locations does not have any significant effect on sound power radiation. But beyond excitation frequency of 200 Hz and when the first peak rises, plate with excitation location 1 shows the highest radiation power of 82 dB in comparison to 79 dB for a plate with excitation locations 2. However, at this forcing frequency of 200 Hz, plate with mid excitation shows the lowest peak sound power level of 78 dB among all excitations. Therefore, it is suggested that plate with mid excitation with parabolically decreasing thickness variation is the lowest sound power radiator among all excitation locations. Further, from Figure 8, it is observed that for a higher forcing region beyond 200 Hz, all acoustic curves due to different taper ratios tends to intersect with each other at this high forcing region for different excitation locations. Figure 9 shows the analytical and numerical comparison of radiation efficiency ( $\sigma_{mn}$ ) for uniform plate having parabolically decreasing thickness variation. A well and good agreement of results is seen in comparison of radiation efficiency as reported in Figure 9. Figure 10 shows the Numerical comparison of radiation efficiency ( $\sigma_{mn}$ ) for circular annular plate having parabolically decreasing thickness variation with different taper ratio  $T_x$  under excitation 1. It is investigated that for a plate with parabolic decreasing thickness, the effect of radiation efficiency due to different taper ratios is independent of exciting frequency rises 100 Hz, but at a given forcing frequency higher taper ratio causes higher radiation efficiency beyond 200 Hz. However, sound power level peaks do shift towards lower frequency as taper ratio increases. For higher frequency beyond 200 Hz, different taper ratios alter its stiffness at higher forcing frequency and the radiation efficiency curve tends to intersect each other at this high forcing region. It is interesting to note that the radiation curve tends to unity in the frequency band 5800 - 6200 Hz and a clear peak are seen in this frequency band for all combinations of acoustic curve due to different taper ratios. Figure 11 shows the Numerical comparison of radiation efficiency ( $\sigma_{mn}$ ) for circular annular plate having parabolically decreasing thickness variation for different excitation locations for taper ratios  $T_x = 0.75$ . From Figure 11 it is observed that for a higher forcing region beyond 200 Hz, mid excitation has lowest radiation efficiency in comparison to other excitations and all radiation efficiency curve due to different taper ratios tends to intersect with each other at this high forcing region for different excitation locations.

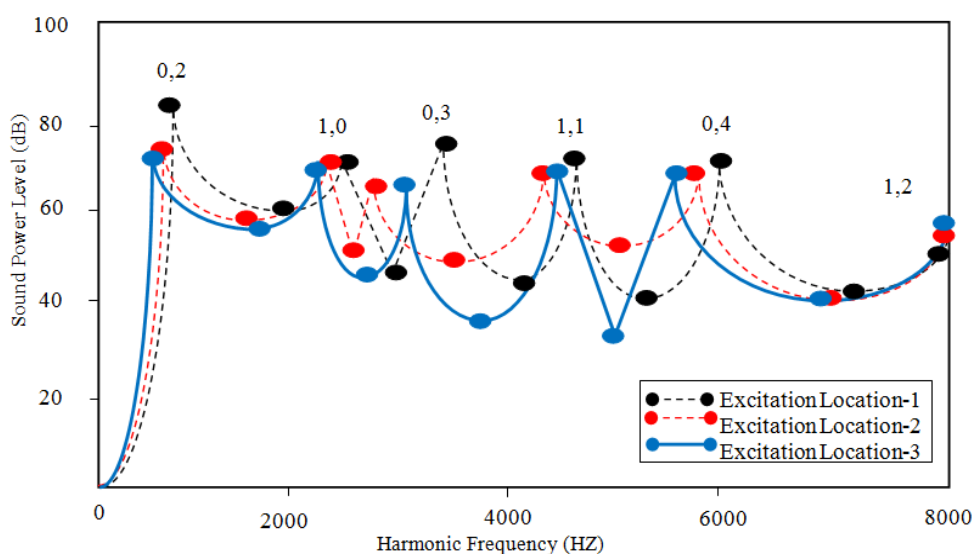


**Figure 8: Numerical Comparison of Sound Power Level for Circular Annular Plate Having Parabolically Decreasing Thickness Variation for Different Excitation Locations for Taper Ratios  $T_x = 0.75$**

### Peak Sound Power Level Variation with Different Taper Ratio for All Excitation Locations

Peak sound power levels due to self and mutual radiation for circular annular plate having parabolic decreasing thickness variation for different taper ratio are shown in Figure 12. Peak sound power level for all excitation locations is reported at first peak which corresponds to (0, 2) mode of the plate. It is clear from Figure 12 that for plate under excitation location 1 i.e. towards outer radius, peak sound power level increases for increasing value of taper ratio whereas for excitation location 2 i.e. towards inner radius, the peak sound power level decreases for increasing taper ratio. When excitations moves towards mid position, then for increasing taper ratio, peak is minimum at  $T_x = 0.50$  and maximum at  $T_x = 0.25$ . It is thus quite obvious that excitation location has significant impact on the peak sound power level. A further excitation location with a different taper ratio provides us design options for peak sound power level. As for example, for peak sound power suppression, plate with taper ratio  $T_x = 0.50$  with mid excitation may be the option. Similarly for sound power actuation, plate with a taper ratio  $T_x = 0.75$  with excitation location 1 towards outer radius may be another alternative solution.

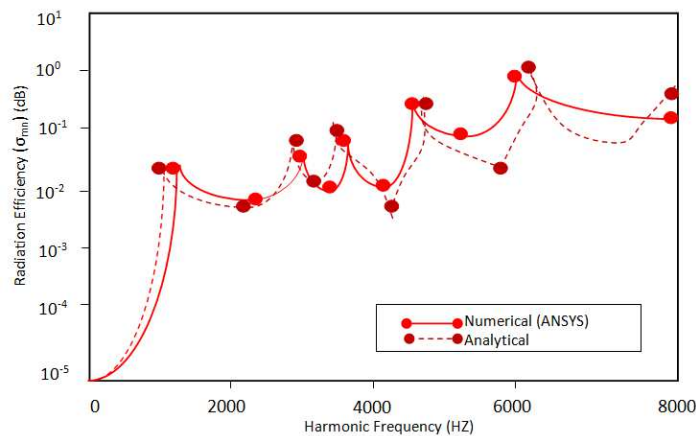


**Figure 9: Analytical and Numerical Comparison of Radiation Efficiency ( $\Sigma_{mn}$ ) for Uniform Plate**

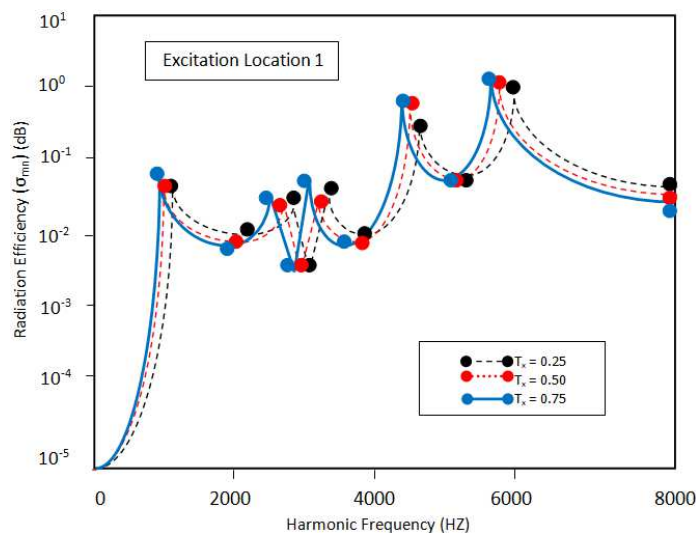


**Figure 10: Numerical Comparison of Radiation Efficiency ( $\Sigma_{mn}$ ) for Circular Annular Plate Having Parabolically Decreasing Thickness Variation with Different Taper Ratio  $T_x$  Under Excitation 1**

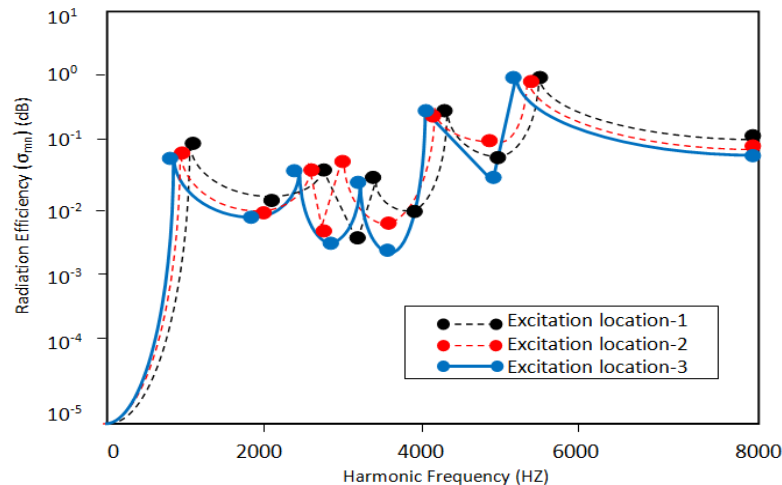


**Figure 11: Numerical Comparison of Radiation Efficiency ( $\Sigma_{mn}$ ) for Circular Annular Plate Having Parabolically Decreasing Thickness Variation for Different Excitation Locations for Taper Ratios  $T_x = 0.75$**

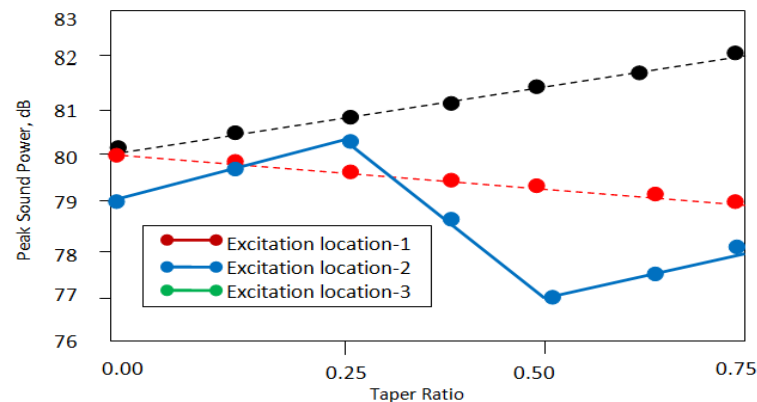


**Figure 12: Peak Sound Power Level (dB) for Plate Having Parabolically Decreasing Thickness Variation**

## CONCLUSIONS

The sound radiation behaviour due to self and mutual radiation of an annular circular plate having parabolically decreasing thickness variation in the air medium with different taper ratio is analysed. It is observed that excitation locations and modes variation have significant impact on sound power level in comparison to the stiffness variation due to taper ratio. For taper ratio  $T_x = 0.75$ , the highest sound power level, 82 dB is obtained for excitation location 1 (towards the outer radius) while for excitation locations 2 (towards the inner radius) and 3 (mid excitation location), the highest sound power level obtained are 79 dB and 78 dB respectively. Further, it obtained that sound power level rises 40 dB, we do not get any design option for excitation location 1 whereas excitation location 3 may be an alternative for sound power level rises 40 dB. For sound power level between (40-50) dB, we get a broad range of frequencies as design options in different frequency bands for different taper ratios at these three excitation locations. It is further investigated that peak sound power level of plate for excitation location 1 increases for increasing value of taper ratio whereas for excitation location 2, peak sound power level decreases for increasing taper ratio. But for mid excitation, the peak sound power level is minimum at  $T_x = 0.50$  and maximum at  $T_x = 0.25$ . It is inferred that excitation locations with a different taper ratio provide us design options for peak sound power level. As, for example, for peak sound power suppression, plate with a taper ratio  $T_x = 0.50$  with mid excitation may be the option. Similarly for sound power actuation, plate with a taper ratio  $T_x = 0.75$  with

excitation location 1 towards the outer radius may be another alternative solution.

## REFERENCES

1. Wang, C. M., Hong, G. M., Tan, T. J. (1995). Elasting buckling of tapered circular plates. *Computers & structure* 55(6), 1055-1061.
2. Gupta, A. P., Goyal, N. (1999). Forced asymmetric response of linearly tapered circular plates. *Journal of sound and vibration* 220(4),641-657.
3. Laura, P. A. A., Gutierrez, R., Sonzognit, H., V., Idelsohn, S. (1997). Buckling of circular, annular plates of non uniform thickness. *Ocean Engineering* 24(1),51-61.
4. Sharma, S., Lal, R., Neelam. (2011). Free transverse vibrations of non-homogeneous circular plates of linearly varying thickness. *Journal of international academy of physical sciences* 15(1),187-200.
5. Wang, C.Y. (2014).The vibration modes of concentrically supported free circular plates. *Journal of sound and vibration* 333(3),835-847.
6. Singh, B, Hassan, S.M. (1998).Transverse vibration of a circular plate with arbitrary thickness variation. *International journal of Mechanical Science* 40(11),1089-1104.
7. Duan, W.H., Wang, C.M., Wang, C.Y. (2008). Modification of fundamental vibration modes of circular plates with free edges. *Journal of Sound and Vibration* 317(3-5),709–715.
8. Gupta, U.S., Lal, R., and Sharma, S. (2007). Vibration of non-homogeneous circular Mindlin plates with variable thickness. *Journal of Sound and Vibration* 302(1-2),1-17.
9. Kang, J.H. (2003). Three-dimensional vibration analysis of thick, circular and annular plates with nonlinear thickness variation. *Computers & Structure* 81(16),1663-1675.
10. Lee, H., Singh, R. (2005). Acoustic radiation from out-of-plane modes of an annular disk using thin and thick plate theories. *Journal of Sound and Vibration*, 282 (1-2),313–339.
11. Thompson Jr., W. (1971). The computation of self- and mutual-radiation impedances for annular and elliptical pistons using Bouwkamp integral. *Journal of Sound and Vibration*, 17 (2),221–233.
12. Levine, H., Leppington, F.G. (1988). A note on the acoustic power output of a circular plate. *Journal of Sound and Vibration*, 121 (5),269–275.
13. Rdzanek Jr., W.P., Engel, Z. (2000). Asymptotic formula for the acoustic power output of a clamped annular plate. *Applied Acoustics*, 60 (1),29–43.
14. Kesavarao, Y., Ramakrishna, C., & Arji, A. (2015). Stress Analysis of Laminated Graphite/Epoxy Composite Plate Using FEM.
15. Wodtke, H.W., Lamancusa, J.S. (1998). Sound power minimization of circular plates through damping layer placement. *Journal of Sound and Vibration*, 215 (5), 1145–1163.
16. Wanyama, W. (2000). Analytical Investigation of the acoustic radiation from linearly-varying circular plates, Doctoral Dissertation, Texas Tech University, Lubbock, USA.
17. Lee, H., Singh, R. (2005). Self and mutual radiation from flexural and radial modes of a thick annular disk. *Journal of Sound and Vibration*, 286(4-5),1032–1040.

18. Cote, A.F., Attala, N., Guyader, J.L. (1998). Vibro acoustic analysis of an unbaffled rotating disk. *Journal Acoustical Society of America*, 103 (3),1483-1492.
19. Jeyraj, P. (2010). Vibro-acoustic behavior of an isotropic plate with arbitrarily varying thickness. *European Journal of Mechanics A/Solids*, 29(6),1088-1094.
20. Ranjan, V., Ghosh, M.K. (2005). Forced vibration response of thin plate with attached discrete dynamic absorbers. *Thin walled structures*, 43(10),1513-1533.
21. Kumar, B., Ranjan, V., Azam, M.S., Singh, P.P., Mishra, P., Ajit, K.P., Kumar. P. (2016). A comparison of vibro acoustic response of isotropic plate with attached discrete patches and point masses having different thickness variation with different taper ratios *Shock and vibration*, Article ID 8431431.
22. Lee, M.R., Singh, R. (1994). Analytical formulations for annular disk sound radiation using structural modes. *Journal of the Acoustical Society of America*, 95 (6),3311–3323.
23. Rdzanek, W.J., Rdzanek W.P.JR. (1997). The real acoustic power of a planar annular membrane radiation for axially-symmetric free vibrations. *Archives of Acoustics*, 22(4),455-462.
24. Mohsin, N. R. (2015). Comparison between Theoretical and Numerical Solutions for Center, Single Edge and Double Edge Cracked Finite Plate Subjected to Tension Stress. *International Journal of Mechanical and Production Engineering Research and Development (IJMPERD)*, 5(2), 11-20.
25. Nakayama, I., Nakamura, A., Takeuchi, R. (1980). Sound insulation of a circular plate for a single sound pulse. *Acustica*, 46(3),330-340.
26. Lee, H., and Singh, R. (2004). Determination of sound radiation from a simplified disk brake rotor using a semi-analytical method *Noise Control Engineering Journal*, 52 (5), 1024-1030
27. Squicciarini, G., Thompson, D.J., Corradi, R. (2014). The effect of different combinations of boundary conditions on the average radiation efficiency of rectangular plates. *Journal of Sound and Vibration*, 333(17),3931–3948.
28. Xie, G., Thompson, D.J., Jones, C.J.C. (2005). The radiation efficiency of baffled plates and strips. *Journal of Sound and Vibration*, 280(1-2),181–209.
29. Rayleigh, J.W. (1948). *The Theory of Sound*, 2nd edition, Dover. New York, USA.
30. Maidanik, G. (1962). Response of ribbed panels to reverberant acoustic fields. *Journal of the Acoustical Society of America*, 34(6),809–826.
31. Heckl, M. (1977). Radiation from plane sound sources. *Acustica*, 37(3),155–166.
32. Williams, E.G. (1983). A series expansion of the acoustic power radiated from planar sources. *Journal of the Acoustical Society of America*, 73(5), 1520–1524.
33. Mohan, P., Suganya, G. S., & Sivanandhan, T. (2014). Pv/Battery to the Grid Integration of Hybrid Energy Conversion System with Power Quality Improvement Issues. *ISSN (E)*, 2321-8843.
34. Keltie, R.F., Peng, H. (1987). The effects of modal coupling on the acoustic power radiation from panels. *Journal of Vibration Acoustics Stress and Reliability in Design*, 109(1), 48–55.
35. Snyder, S.D., Tanaka, N. (1995). Calculating total acoustic power output using modal radiation efficiencies. *Journal of the Acoustical Society of America*, 97(3),1702–1709.